Strategic locus for the activation of the superoxide dismutase gene in the nephron

SHIGERU KIYAMA, TOSHIMASA YOSHIOKA, IAN M. BURR, VALENTINA KON, AGNES FOGO, and IEKUNI ICHIKAWA

Departments of Pediatrics and Pathology, Vanderbilt University School of Medicine, Nashville, Tennessee, USA

Strategic locus for the activation of the superoxide dismutase gene in the nephron. Upon exposure to a transient ischemia, the distal tubule of the kidney often escapes the severe damage which afflicts the proximal tubule. To ascertain whether this feature of the distal tubule is attributable to its intrinsic cellular properties, we focused on two pairs of unique tubule segments; distal versus proximal convoluted tubules in the superficial cortex and distal versus proximal straight tubules in the outer stripe of the outer medulla. These tubules were chosen because, firstly, they can be identified by morphology and immunostaining, and secondly, each pair has the same anatomical relationship to the circulation. Detailed morphometric analyses were performed six hours following unilateral transient ischemia in adult rats to semiquantitate the local tissue damage in these specific nephron segments. The architecture of the distal convoluted and straight tubules was remarkably well preserved, contrasting to the moderate to extensive necrotic changes seen in the proximal tubules. In search of the potential intrinsic cellular mechanism that underlies the observed difference, we examined the segmental distribution along the nephron of manganese superoxide dismutase gene transcripts by *in situ* hybridization. This antioxidant enzyme gene was expressed primarily in the distal tubules with contrastingly low levels of expression in the proximal tubules. Moreover, following ischemia-reperfusion, this distal tubule-dominant pattern was further accentuated immediately following reperfusion. The study indicates that the marked difference between the proximal and distal tubules in their susceptibility to injury *in vivo* is attributable to their intrinsic cellular properties, which include the local level of antioxidants.

Kidneys exposed to a transient ischemic insult develop a highly heterogenous pattern of tissue damage [1–4]. Proximal 'straight' tubules (in contrast to 'convoluted' tubules) are prone to develop necrosis even after renal arterial clamping of short duration [1, 2]. Since the proximal straight tubule (PST) is located in the outer medulla and medullary rays, which are low in oxygen tension [5], it has been suggested that a variability in the degree of local hypoxia, being most marked in the straight tubule, underlies heterogenous injury within the proximal tubule [6]. Thus, it has been postulated that the geographic proximity of the proximal nephron segment to the vascular structure determines the extent of injury, as it dictates the supply and availability of oxygen to the segment [6–9].

It has also been noted that distal tubules are less susceptible to injury following transient ischemia than the proximal [3, 4, 6, 10]. This phenomenon becomes of greater significance when one considers the fact that distal tubules have higher Na^+-K^+-ATPase activity and consequent greater oxygen demand than the proximal [11]. In considering the mechanism underlying this strategically sound, high resistance to injury of the distal tubules which allows maintenance of body fluids in the face of proximal tubule damage via tubuloglomerular feedback and adjusted reabsorption [12, 13], one realizes that the proximal and distal tubules, for the most part, do not share a comparable geographic relationship to the vasculature. The exceptions are the superficial cortex (for the convoluted tubules) and the outer stripe of the outer medulla (for the straight tubules) [14, 15]. Examination of the two tubules at these unique sites, therefore, allows evaluation of the contribution of factors intrinsic to the tubule cells in their susceptibility to injury.

Of the potentially extensive list of intrinsic factors contributory to the remarkable resistance of the distal tubule, we focused in the present study on manganese superoxide dismutase (Mn-SOD). In addition to numerous indirect experimental data suggestive of the functionally significant role of this antioxidant enzyme in affecting a variety of renal injuries [16, 17], a most recent study [18[1]] using transgenic mice carrying the human SOD gene provided, although in preliminary fashion, unequivocal evidence to indicate that this enzyme has a crucial impact on the degree of renal tissue damage which follows a transient ischemia. While Cu/Zn-SOD is considered to be constitutive, Mn-SOD has been shown *in vitro* to be inducible by several forms of oxidants in renal [19] and non-renal cells [20, 21]. In a most recent study in animals [17], transient renal ischemia and reperfusion led to activation of this antioxidant enzyme, which paralleled acquisition by the kidney of effective tolerance against ischemia-reperfusion and other oxidant-induced injuries. Of note, a previous study demonstrated that the local levels of several other antioxidant enzymes are rather higher in the proximal than distal tubules [22].

We, therefore, sought to ascertain in the present study whether, with the anatomical relationship of the tubule segment to the vasculature strictly controlled, the level and the response of the activity of this gene potentially underlies the magnitude of local protection from injury caused by ischemia-reperfusion.

---

[1] The study has not been completed as a full-scale investigation due to unavailability of the transgenic mouse.

Methods

Animals

Adult male Munich-Wistar rats (body wt 200 to 264 g) were studied. They were fed normal rat chow and allowed free access to tap water during the study. Rats were anesthetized with sodium pentobarbital (50 mg/kg body wt, intraperitoneally) for surgical procedures.

Induction of transient ischemia

In 13 rats, a transient ischemia was induced in the left kidney, following the protocol employed previously by us to impose on the kidney a typical ischemia-reperfusion insult [17]. The right kidney was untouched to serve as a control. Briefly, after anesthesia, animals were placed on a heated table and laparotomy was performed exposing the left renal artery; a hemostatic clamp was applied on the left renal artery for 30 minutes to create a complete renal ischemia. The clamp was then removed; prompt reperfusion was assured by visual inspection of the kidney surface, and the abdominal incision was closed. Three ($N = 3$) or six hours ($N = 10$) after removal of the clamp, both kidneys were harvested under anesthesia. Perfusion fixation was carried out as described below to prepare tissues for *in situ* hybridization in three animals from each time point. Kidneys from the remaining seven rats with six hours of reperfusion were immersion fixed in 4% paraformaldehyde (PFA) and processed routinely. Three μm thick sections were stained with H & E or PAS and examined by light microscopy.

In situ *hybridization studies*

Probe for in situ *hybridization.* To synthesize riboprobe, a 1 k base-pair (bp) EcoR I /Pst I rat Mn-SOD cDNA fragment containing the entire protein coding region and 360 bp of the 3'-nontranslated exon [23] was subcloned into the pGEM-4Z vector, allowing the generation of both sense and antisense cRNA probes. After linearization of the plasmid by pertinent restriction enzymes, sense and antisense cRNA of Mn-SOD were synthesized by using RNA polymerases with ^{35}S-UTP in the reaction mixture. Sense cRNA was used as a negative control. Prior to *in situ* hybridization, limited alkaline hydrolysis was used to cut probes to an average length of ~200 bp [24], which was confirmed by gel electrophoresis.

In situ *hybridization. In situ* hybridization studies were performed in seven normal rats and six rats exposed to a transient ischemia. After anesthesia, rats were perfused *in vivo* via the left cardiac ventricle with 20 ml PBS followed by 20 ml of 4% PFA in phosphate buffer (pH 7.4) [25]. Kidneys were harvested and placed overnight in 4% PFA at 4°C, processed routinely, embedded in paraffin, and stored at 4°C until hybridization studies. Four μm thick tissue sections were then made and placed on 2% 3-aminopropyltriethoxysilane-coated glass slides. Sections were dewaxed in xylene, then hydrated serially in 100% to 30% ethanol. They were refixed in 4% PFA for 20 minutes, washed with PBS, and then treated with 20 μg/ml proteinase K in 50 mM Tris-HCl, pH 7.4, and 5 mM EDTA for 10 minutes. Subsequently, sections were treated with 0.1 M triethanolamine, 0.4% (vol/vol) acetic anhydride for 10 minutes, followed by addition of 0.4% (vol/vol) acetic anhydride for 10 minutes. After rinsing in PBS, sections were successively dehydrated in 30% to 100% ethanol and air-dried.

Two $\times$ 10^6 cpm/slide of ^{35}S-labeled cRNA for Mn-SOD and ^{35}S-labeled control probes were used. Approximate volume per slide of hybridization mixture was 100 μl. Hybridization buffer contained 50% deionized formamide, 10% dextran sulfate, 8 mM DTT, 0.2 mg/ml tRNA and 1 $\times$ salts (300 mM NaCl, 10 mM Tris-HCl, 5 mM EDTA, 0.02% polyvinylpyrolidone, 0.02% Ficoll and 0.02% BSA). Sections were incubated overnight at 50°C in a sealed humidified container. Subsequently, sections were washed in 50% deionized formamide, 2 $\times$ SSC (300 mM NaCl, 30 mM sodium citrate, pH 7.0), 100 mM DTT at 65°C for 20 minutes, followed by TEN buffer (10 mM Tris-HCl, 5 mM EDTA and 500 mM NaCl) at 37°C, and treated with 20 μg/ml RNase at 37°C for 30 minutes. Sections were washed in 2 $\times$ SSC, followed by 0.1 $\times$ SSC at 65°C, dehydrated in 30% to 100% ethanol with 0.3 M ammonium acetate, and air-dried. They were dipped in photographic emulsion diluted in 2% glycerol solution, air-dried for 20 minutes, and exposed at 4°C for 7 to 10 days. The sections were developed with D-19 developer and counterstained with toluidine blue.

Quantitative analysis of in situ *hybridization.* Local expression of Mn-SOD mRNA was quantitated by counting the number of silver grains over areas of tissue sections. Individual grains were counted for 20 randomly chosen tubule segments on a single section, which had been hybridized with an antisense cRNA probe, and for 10 tubule segments on a single section hybridized with a sense cRNA probe. Areas of tubular epithelia were quantitated with a computerized planimeter by tracing the outline of tubules and lumens. The density of the signal was expressed in two ways, namely grains/μm^2 and grains/cell [26]. These indices were calculated by counting the grains within specific tubule segments, which were then standardized by the area (μm^2) and by the number of cell nuclei, respectively. The signal density was determined for the superficial cortex and the outer stripe of the outer medulla separately. Mean values for proximal and distal tubules were obtained for individual animals, both normal and post-ischemic rats. Since meaningful quantitation of mRNA message cannot be achieved after establishment of tissue damage, we performed *in situ* hybridization studies within three hours of reperfusion (detailed protocol discussed above). In our pilot studies, we found, as have many other investigators, that practically no light-microscopically appreciable tissue damage develops within three hours of reperfusion.

Semi-quantitation of ischemia-reperfusion injury per tubule segment

To achieve a quantitative comparison of the degree of tissue damage between tubule segments, frank tubular necrosis (cell detachment from the tubular basement membrane, cell fragmentation, loss of nuclear detail) [27] was assessed for proximal and distal tubules and results expressed as percentage of segments affected. Non-overlapping contiguous adjacent 40 $\times$ fields were examined. A section from the contralateral kidney was used as a control.

Identification of specific tubule segments for study

Pairing of tubule segments for study. In testing the functional significance of the intrinsic cellular mechanism(s) on local tissue damage, independent of the local oxygen supply, we selected two unique pairs of tubule segments that not only can be identified by
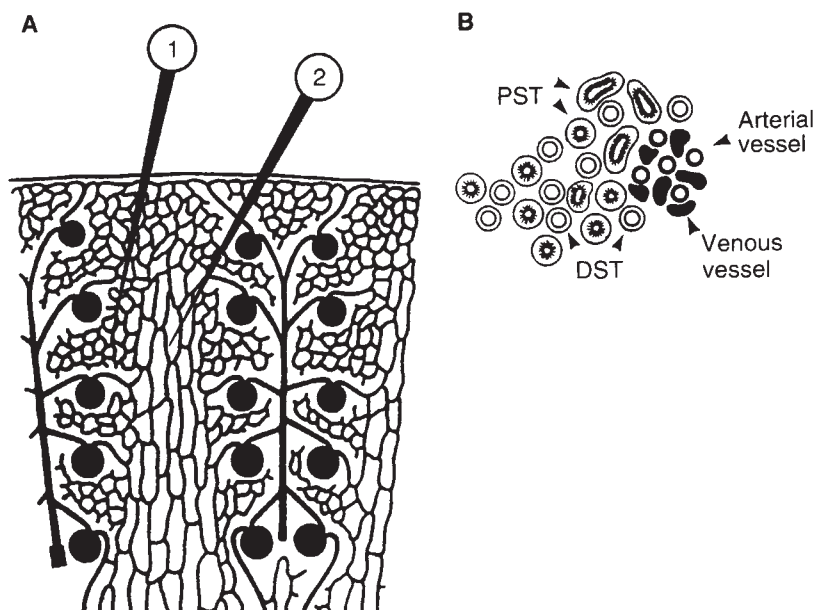
Fig. 1. A. *The anatomical arrangement of the arterial microvascular trees within the superficial cortex.* Within the superficial cortex, two distinctive patterns of the capillary network exist (*arrows 1 and 2*). Within a given network pattern, proximal and distal convoluted tubules are equally embedded in the dense capillary plexus of the labyrinth (*arrow 1*). (Adapted from Kriz W, Lever AF: Renal countercurrent mechanisms: Structure and function. *Am Heart J* 78:101–118, 1969; used with permission). **B.** Geographic relationship between tubules and vasculature in a cross section of the outer stripe of the outer medulla. Proximal straight tubules (PST) and distal straight tubules (DST) have the same proximity to the vascular supply at the level of the outer stripe. (Adapted from Koushanpour E, Kriz W: *Renal physiology. Principles, Structure and Function.* New York, Springer-Verlag, 1986; used with permission)

light microscopy but also have identical geographic relationships to the vasculature. Within the cortex, two distinctive patterns of the capillary network exist (that is, the dense capillary plexus of the cortical labyrinth and the less dense plexus of the medullary rays) [14] (Fig. 1A). Within the superficial cortex, proximal convoluted tubules (PCT) and distal convoluted tubules (DCT) are embedded in the dense capillary plexus of the labyrinth in an identical fashion [14]. Therefore, we selected PCT and DCT in the superficial cortex as the first pair of tubule segments for our comparative study. The pair of proximal (PST) and distal (DST) straight tubules residing within the outer stripe of the outer medulla was selected as the second pair of tubule segments for our investigation. Within this area, PST and DST are distributed in the same manner with regard to their anatomical relationship to the vascular bundles [14, 15] (Fig. 1B).

Morphologic criteria for identification and their verification by immunostaining. Tubules which reside within the cortex include PCT, DCT, DST (or cortical thick ascending limb), connecting tubules (CNT), and collecting ducts (CD). Proximal tubules were distinguished from other segments by characteristic brush border and their relatively large epithelial cell bodies. The distal tubules (DCT and DST) show a striae-like staining within the cells reflecting an extensive formation of lamella-like lateral processes containing large mitochondria [14], whereas CD show a relatively weak and homogeneous staining. In addition, DCT has taller epithelia than DST or CD, and show apical nuclei often with flattening [14]. Since the CNT cells share some morphologic features with DCT cells as well as CD cells, and since the transition from CNT to DCT or CD is not sharp in the rat, distinguishing DCT from CNT under light microscopy may potentially be ambiguous [14, 15]. Within the outer stripe of the outer medulla, there are three different tubule segments, namely, PST, DST (or medullary thick ascending limb) and CD [14, 15], identified as above. To validate our light microscopic method of identifying distal tubules, immunostaining was performed in serial sections immediately adjacent to the sections which were used for *in situ* hybridization or morphologic analyses of tubular injury. A

goat anti-human Tamm-Horsfall protein (THP) antibody (a specific marker for DST) [28] and mouse monoclonal anti-rabbit CD antibody [28, 29] were employed for immunostaining. After tissue sections were incubated with the anti-THP or anti-CD antibody, they were treated with either a biotinylated rabbit anti-goat or horse anti-mouse secondary antibody. Immunolabeling was visualized by using an avidin-biotin horseradish peroxidase labeling kit and diaminobenzidine reaction. Sections were counterstained by PAS or toluidine blue. As a control, some sections were incubated with either nonspecific goat or mouse IgG at the same protein concentrations. No immunolabeling was detected in these sections (not shown). In pilot studies, anti-rabbit CD antibody reacted only with segments morphologically identified as CD in normal rat.

Reagents and instruments

Rat Mn-SOD cDNA was kindly provided by Dr. Harry Nick of the University of Florida, College of Medicine (Gainesville, FL, USA). RNA polymerases and pGEM-4Z vector were obtained from Promega (Madison, WI, USA). ^{35}S-UTP came from DuPont (Boston, MA, USA). Goat anti-human Tamm-Horsfall protein antibody was purchased from Organon Teknika (Durham, NC, USA). Mouse monoclonal anti-rabbit collecting duct antibody was provided by Dr. Matthew D. Breyer (Vanderbilt University, Nashville, TN, USA). Avidin-biotin horseradish peroxidase labeling kit was from Vector Laboratories (Burlingame, CA, USA). Computerized planimeter Micro-plan II was obtained from Donsanto Corp. (Natick, MA, USA). Photographic emulsion was obtained from Polysciences Inc., (Warrington, PA, USA). D-19 developer was from Kodak (Rochester, NY, USA). Other chemicals were obtained from Sigma (St. Louis, MO, USA).

Statistics

All values are expressed as the mean ± SE. Paired *t*-test was performed for statistical comparison between proximal and distal tubules. $P < 0.05$ was considered to be statistically significant.
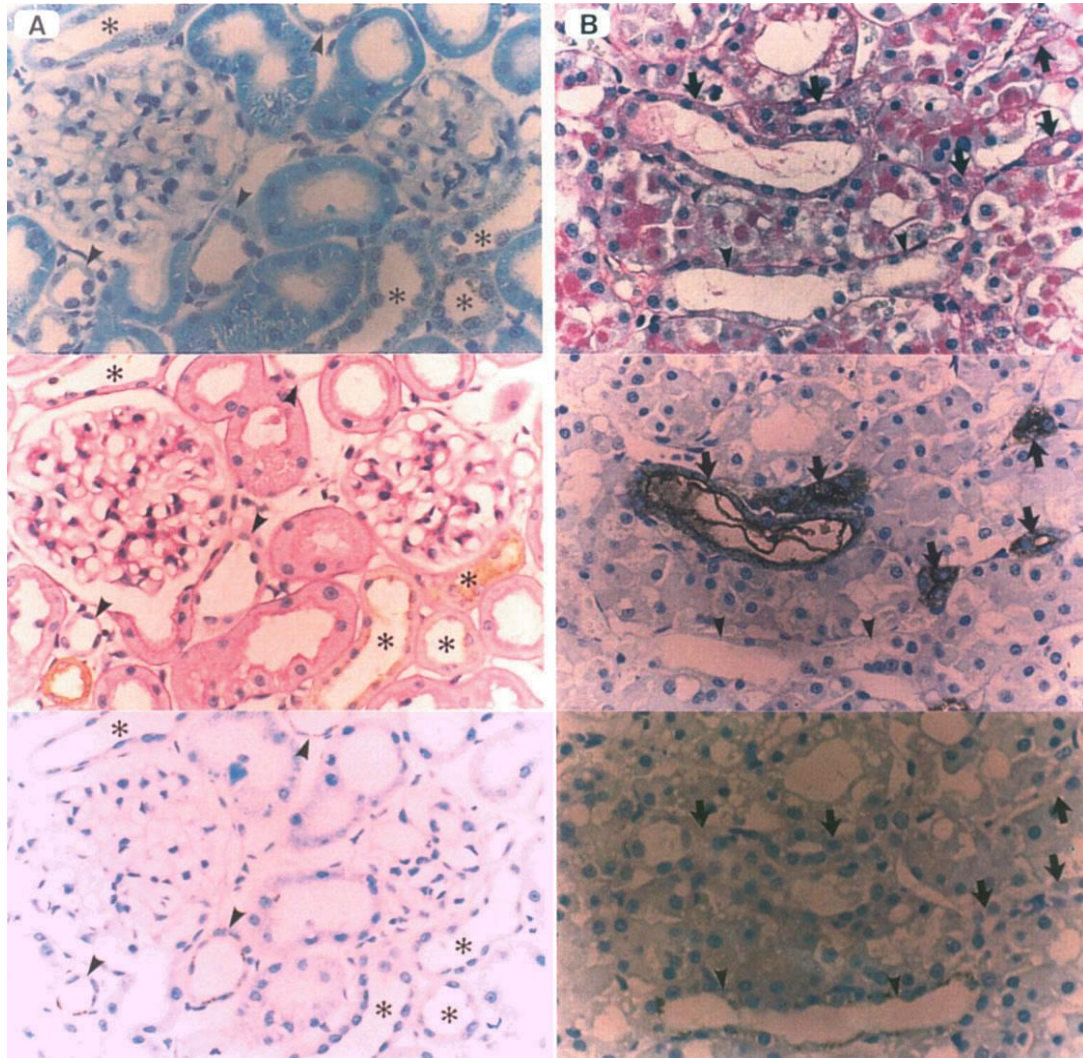
Fig. 2. *Photomicrographs of serial sections from the superficial cortex of a normal rat kidney* (**A**) *and the outer stripe of the outer medulla of a rat kidney exposed to 30 minute ischemia followed by 6 hour reperfusion* (**B**). To validate our light microscopic method of identifying distal tubules, immunostaining was performed in serial sections immediately adjacent to the sections which were used for *in situ* hybridization or morphologic analyses of tubule injury. Sections adjacent to the section hybridized with antisense Mn-SOD cRNA (*A, top*) or to the section used for analysis of tubular damage (*B, top*) were immunostained with anti-human Tamm-Horsfall protein (THP) antibody, a specific marker for distal straight tubules (*middle*), or anti-rabbit collecting duct (CD) antibody (*bottom*). Within the superficial cortex, distal convoluted tubule cells (*asterisks*) did not stain with either anti-THP antibody (*A, middle*) or anti-CD antibody (*A, bottom*), though a weak staining for THP can be observed within their lumen (*A, middle*). Epithelial cells of CD (*arrowheads*) showed coarse granular staining with anti-CD antibody (*A, bottom*). In the outer stripe of the outer medulla, identification of distal straight tubules (*arrows*) was verified by positive cellular staining with anti-THP antibody (*B, middle*) or negative staining with anti-CD antibody (*B, bottom*). Epithelial cells of CD (*arrow heads*) showed coarse granular staining with anti-CD antibody. (PAS or toluidine blue stain, ×300)

Results

Validation of the identification of tubule segments

Our light microscopic method of identifying distal tubule segments was verified by a separate series of experiments in which the accuracy of light microscopic identification of distal tubules was assessed using immunostaining patterns as the gold standard. Serial sections were available from several kidneys used for *in situ* hybridization or morphologic analysis of tubule injury (normal rats, $N = 2$; ischemia-3 hr reperfusion, $N = 1$; ischemia-6 hr reperfusion, $N = 2$). One hundred distal nephron segments were randomly selected in either the superficial cortex or the outer stripe of the outer medulla from each animal. After these tubules

were classified as DCT (or CNT), DST, or CD under light microscopy, the identification of tubule segments was disclosed by examining the immunostaining patterns of the immediately adjacent sections (Fig. 2). In the superficial cortex, false positive for the DCT was 2.1%, 4.2%, and 5.9% in kidneys from normal rats, ischemia-3 hour reperfusion, and ischemia-6 hour reperfusion, respectively. False negative for the DCT was 1.0%, 3.8%, and 2.1% in respective kidneys. In the outer stripe of the outer medulla, false positive for the DST was 0%, 0%, and 1.4% in kidneys from normal rats, ischemia-3 hour reperfusion, and ischemia-6 hour reperfusion, respectively. False negative for the DST was 0%, 3.8%, and 6.7% in respective kidneys.
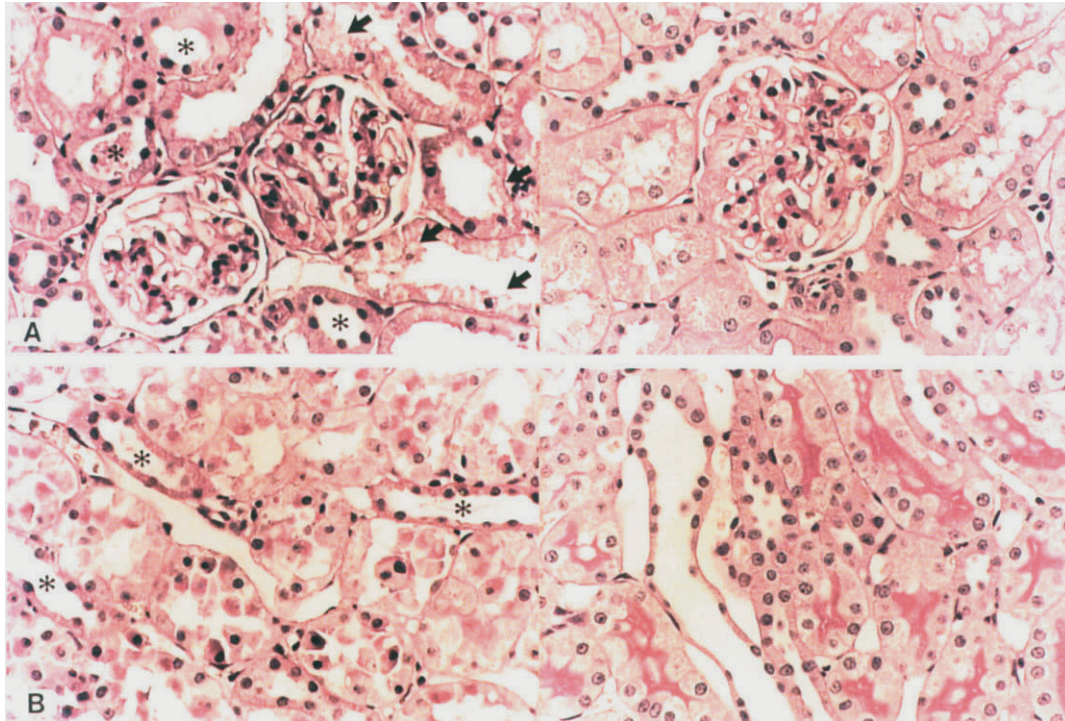
Fig. 3. *Impact of transient ischemia on the morphology of the superficial cortex and the outer stripe of the outer medulla.* In the cortex (**A**, *left*), marked cellular injury, including loss of brush borders, cellular fragmentation, and loss of nuclei, was focally seen in proximal (*arrows*) but not in distal tubules (*asterisks*). In the outer medulla (**B**, *left*), extensive injury, including cellular detachment from basement membrane and cellular fragmentation, was seen in proximal tubules, whereas distal tubules were well preserved (*asterisks*). The light microscopic findings in the corresponding regions of the contralateral undisturbed kidneys are illustrated in the right side panels. (PAS stain, ×300)

Semiquantitative analysis of post-ischemic damage in tubule segments

In the superficial cortex, substantial cellular damage, including loss of brush border, cellular fragmentation, and loss of nuclei, was focally but frequently seen in proximal tubules but rarely in distal tubules (Fig. 3A, left). In the outer stripe of the outer medulla, extensive damage, including cellular detachment from basement membrane and cellular fragmentation, occurred in proximal tubules. In comparison, distal tubules were remarkably well preserved (Fig. 3B, left). To perform quantitative analysis of tissue damage, we assessed the percentage of tubule segments with necrosis in these two regions. It has been shown that, within the cortical labyrinth, there may be a zone of protection from ischemic injury in an area surrounding the arteries [6] and glomeruli [9]. In this regard, we examined PCT and DCT adjacent to the glomeruli observed in 40 × fields along the renal surface in the superficial cortex. On average, 260 PCT (range 198 to 338) and 101 DCT (range 68 to 147) per rat were examined in the superficial cortex. In the outer stripe of the outer medulla, on average, 273 PST (range 253 to 299) and 73 DST (range 57 to 87) per rat were studied. As shown in Figure 4, significantly more extensive tubular necrosis occurred in proximal tubules in both of these areas. Thus, the percentage of tubular necrosis in the proximal versus the distal tubules was 13.8 ± 0.9% versus 0.9 ± 0.3% and 97.1 ± 0.7% versus 5.2 ± 1.2% in the superficial cortex and the outer stripe of the outer medulla, respectively ($P < 0.01$).

In situ *hybridization of normal rat kidneys*

To localize Mn-SOD mRNA, kidneys from normal adult rats were hybridized with antisense Mn-SOD cRNA. Only a weak signal was detectable in the glomerulus and other vascular components. Although, in comparison, higher levels of signal were present in tubule epithelia, the signal was still low in proximal tubules and collecting ducts, whereas intense signals were localized primarily in distal tubules, both within the superficial cortex and the outer stripe of the outer medulla (Fig. 5). Within each distal tubule segment, the distribution of the signal was uniform, occupying homogeneously the entire luminal circumference of the segment. It was difficult to identify the signals on thin limbs due to the limited resolution of light microscopy. Sense cRNA hybridization showed extremely low background and lack of specific cellular labeling. The greater accumulation of Mn-SOD mRNA in distal tubules than in proximal tubules was further verified by a quantitative analysis of local signal density. Thus, as summarized in Figure 6, in the superficial cortex, the density of the signal, expressed as the number of silver grains per area, averaged 0.182 ± 0.032 grains/μm^2 for distal tubules, a value significantly higher than that for proximal tubules (0.044 ± 0.008 grains/μm^2, $P < 0.05$). The value averaged 21.3 ± 0.6 grains/cell for distal tubules, again significantly higher than that for proximal tubules (11.8 ± 1.5 grains/cell, $P < 0.01$). Similarly, in the outer stripe of the outer medulla, the density of the signal averaged 0.200 ± 0.014 grains/ μm^2 and 22.4 ± 1.0 grains/cell, respectively, for distal tubules,
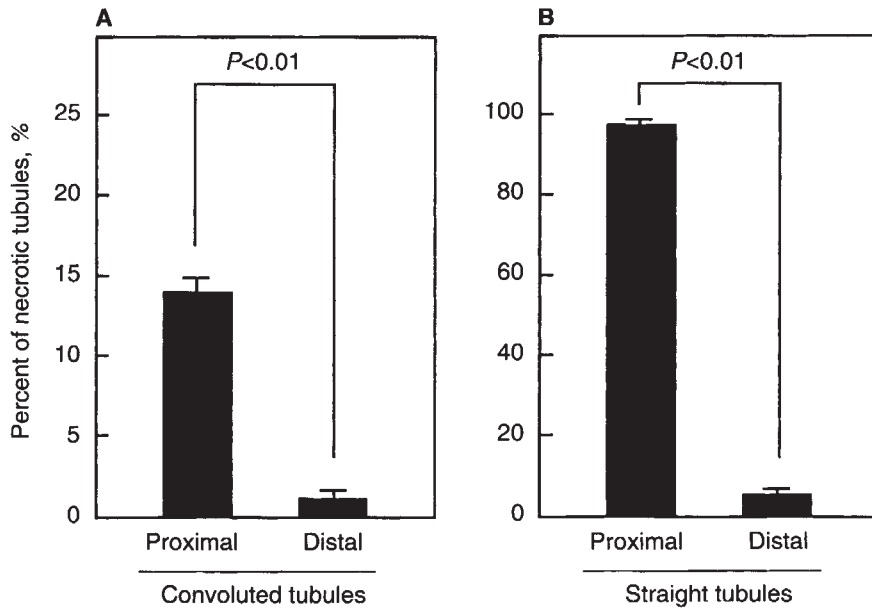
Fig. 4. *Semiquantitative analysis of tubule necrosis.* Tubule necrosis was significantly more extensive in proximal than in distal tubules in the superficial cortex (convoluted tubules) (*left panel*) and the outer stripe of the outer medulla (straight tubules) (*right panel*).
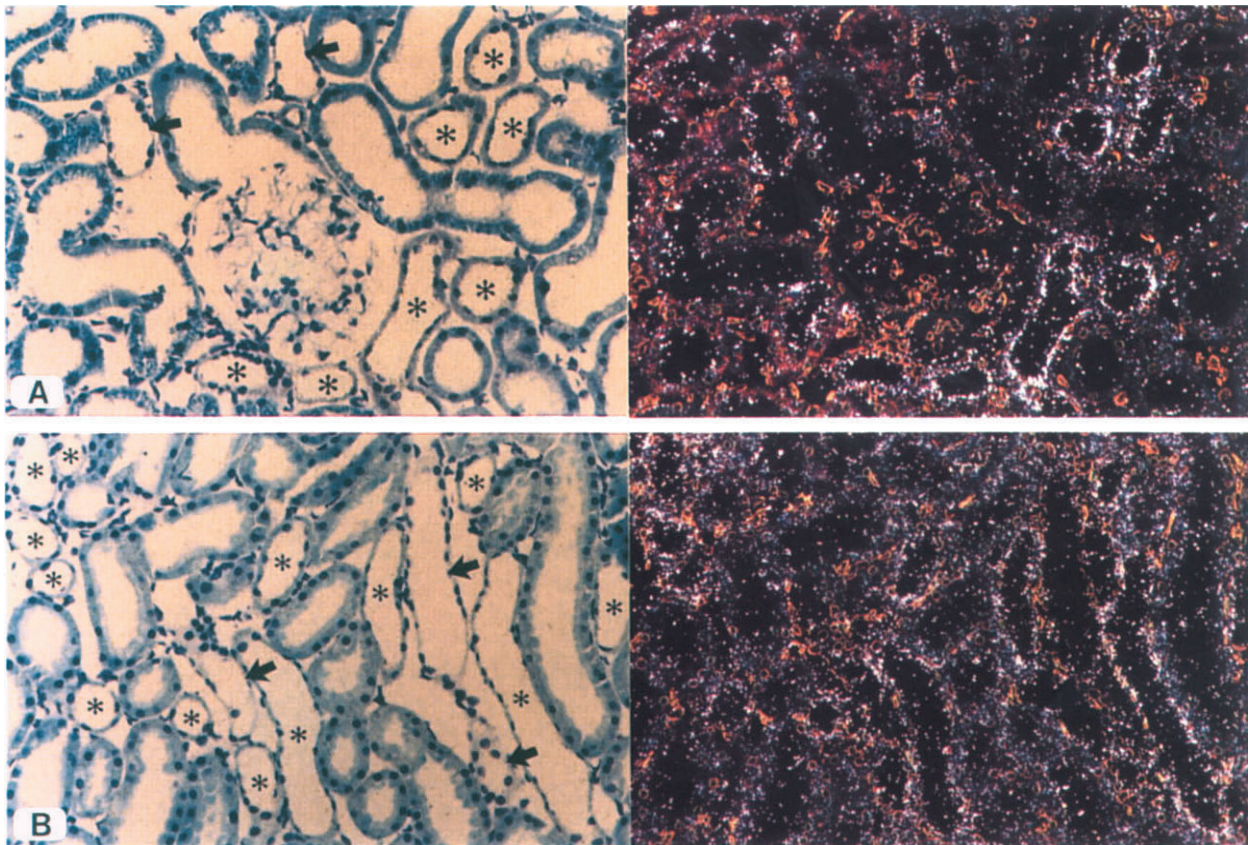

Fig. 5. *Bright* (left) *and dark* (right) *field photomicrographs of the superficial cortex* (**A**) *and the outer stripe of the outer medulla* (**B**) *from normal rat kidneys demonstrating localization of antisense Mn-SOD cRNA.* Within the glomerulus, only a weak signal was detectable. Signals were readily detectable over tubule epithelia. More intense signals were localized in distal tubules (*asterisks*) compared to proximal tubules or collecting ducts (*arrows*). (Toluidine blue counterstain, ×190)

whereas those for proximal tubules were significantly and substantially lower, averaging 0.077 ± 0.007 grains/μm^2 ($P < 0.01$) and 13.2 ± 0.6 grains/cell ($P < 0.01$), respectively. Thus, the signal density was significantly higher in distal tubules compared to proximal tubules in both the superficial cortex and the outer stripe of the outer medulla in normal undisturbed kidneys. These
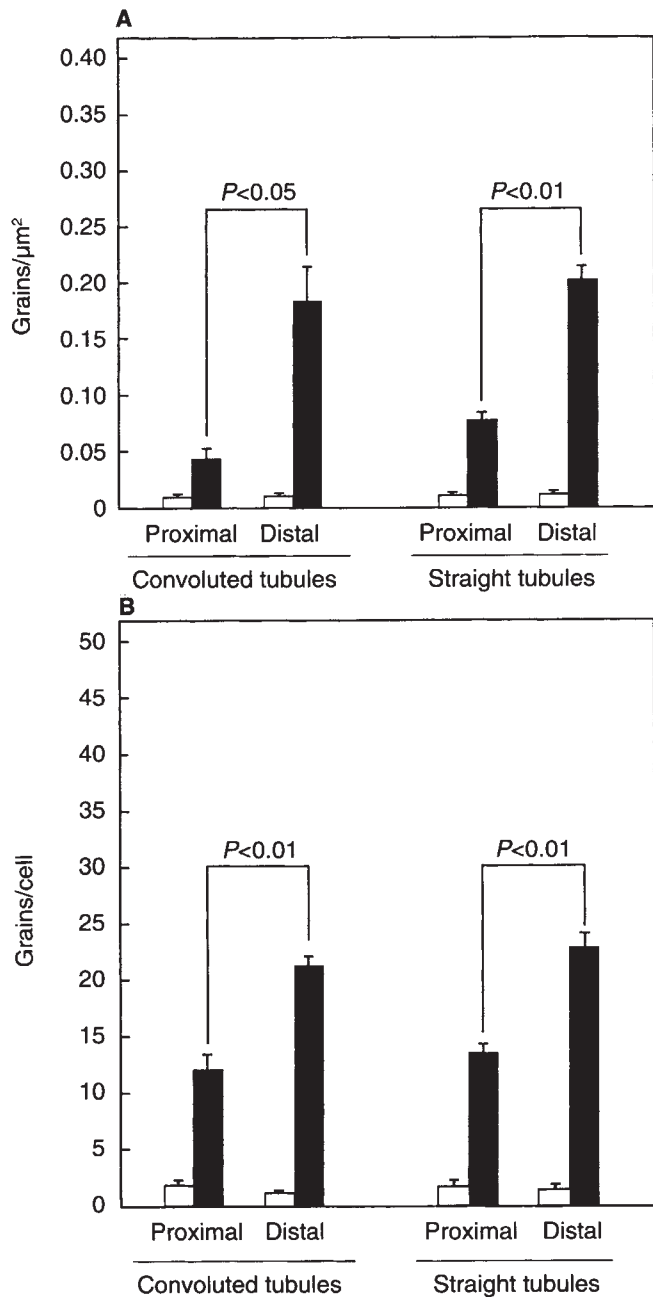
Fig. 6. *Quantitative analysis of Mn-SOD mRNA signals in normal rat kidneys.* Closed bars, density of silver grains in the nephron segments hybridized with antisense cRNA; open bars, those in segments hybridized with sense cRNA. The density of silver grains, expressed as number per area (*upper panel*) and per cell (*lower panel*), was significantly and substantially greater in distal than proximal tubules in the superficial cortex (convoluted tubules) and the outer stripe of the outer medulla (straight tubules).

patterns of preferential distribution of signals along the distal tubule segments were essentially identical in all animals examined. The densities of silver grains in the same tubule segments hybridized with a control sense cRNA were extremely low. Thus, the density of grains in the proximal and distal tubules averaged 0.009 ± 0.002 grains/μm^2 and 0.010 ± 0.002, respectively, in the

superficial cortex and 0.011 ± 0.003 grains/μm^2 and 0.012 ± 0.003, respectively, in the outer stripe of the outer medulla. Likewise, the grains for sense probe per cell in the proximal and the distal tubule averaged 2.0 ± 0.4 grains/cell and 0.9 ± 0.2, respectively, in the superficial cortex and 1.8 ± 0.4 grains/cell and 1.2 ± 0.4, respectively, in the outer stripe of the outer medulla.

In situ *hybridization of kidneys following transient ischemia*

To determine the relative density of Mn-SOD mRNA immediately following transient ischemia, kidneys exposed to 30 minutes of ischemia were harvested three hours and six hours after reperfusion for *in situ* hybridization. The contralateral kidneys served as controls. In these settings, remarkably high levels of signal were detected in distal tubules in both cortex and outer medulla (Fig. 7). The difference in the intensity of signals between the proximal and distal tubules was more apparent in the kidneys exposed to the transient ischemia than in the contralateral undisturbed kidneys (data from contralateral kidneys, not shown, were similar to normal rat kidneys). Quantitation of silver grains was performed in these kidneys. Thus, as summarized in Figure 8, in the superficial cortex, the density of the signal, expressed as the number of silver grains per area, averaged 0.295 ± 0.039 grains/ μm^2 for distal tubules, a value significantly higher than that for proximal tubules (0.050 ± 0.007 grains/μm^2, $P < 0.05$). The value averaged 32.6 ± 3.4 grains/cell for distal tubules, a value again significantly higher than that for proximal tubules (11.5 ± 0.9 grains/cell, $P < 0.05$). Similarly, in the outer stripe of the outer medulla, the density of signal averaged 0.335 ± 0.047 grains/μm^2 and 44.2 ± 4.5 grains/cell, respectively, for distal tubules, whereas those for proximal tubules were significantly and substantially lower, averaging 0.079 ± 0.010 grains/μm^2 ($P < 0.05$) and 13.6 ± 1.4 grains/cell ($P < 0.05$), respectively. The densities of silver grains in the same segments hybridized with a control sense cRNA were extremely low, similar to normal undisturbed kidneys. Thus, the preferential distribution of Mn-SOD mRNA to distal convoluted and straight tubules over the corresponding proximal tubule segments became accentuated shortly after the exposure to transient ischemia. Indeed, for both the superficial cortex and the outer stripe of the outer medulla, the difference in the signal density between proximal and distal tubules was significant and some twofold greater in post-ischemic kidneys when compared to the contralateral kidneys prepared simultaneously from the same animals.

Discussion

Proximal and distal tubules are encompassed by an identical microcirculatory milieu at two specific regions in the kidney, that is, the superficial cortex (for the convoluted tubules) and the outer stripe of the outer medulla (for the straight tubules). These unique anatomical settings provided us with the opportunity to assess the contribution of intrinsic tubule cell properties to their susceptibility to damage in the *in vivo* model of transient ischemia. To achieve our goal, accurate identification of each tubule segment was essential, as described in **Methods.**

Further, the experimental insult of 30 minutes ischemia followed by six hours reperfusion was chosen because it produced the typical post-ischemic morphologic derangements in both proximal and distal tubules, yet the identity of the damaged segments could be made morphologically. Of interest, this protocol has a remarkable resemblance to those of previous studies in
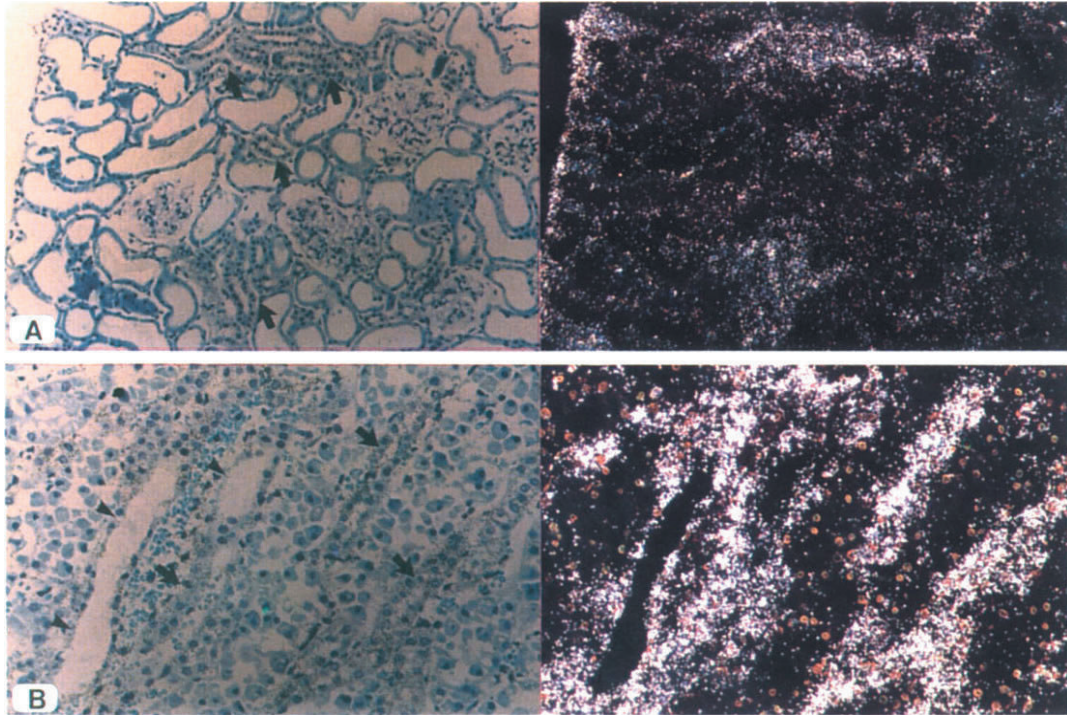
Fig. 7. *Bright (left) and dark (right) field photomicrographs of rat kidneys exposed to a transient ischemia and hybridized with antisense Mn-SOD cRNA.* **A.** Renal cortex exposed to 30 minute ischemia followed by 3 hour reperfusion. **B.** Outer stripe of outer medulla of the kidney exposed to 30 minute ischemia followed by 6 hour reperfusion. A markedly high signal was detectable in distal tubules (*arrows*). The difference in the intensity of signals between the proximal and distal tubules was more accentuated in these injured kidneys than in the contralateral undisturbed kidneys (not shown). Intense signals were detectable in collecting ducts (*arrow heads*), although not as intense as those in the distal tubules. (Toluidine blue counterstain, ×100 (A), ×190 (B)).

which the kidneys of transgenic mice carrying the human SOD gene were found to be resistant to post-ischemic damage [18] and those in which administration of SOD exogenously in rats attenuated the typical renal tissue damage induced by transient ischemia [30]. Apparently, in both mice [18] and rats [31], ischemia of longer duration brings about severe tissue necrosis through mechanisms independent of reactive oxygen metabolites, and distal straight tubules can exhibit severe injury [3, 32].

Our semiquantitative morphologic analysis of tissue damage within the two specific regions points to the existence of highly efficient intrinsic defense mechanism(s) that are prominent in the distal tubule. An intrinsic mechanism underlying the heterogeneous tolerance to ischemic insult within the proximal tubule was previously proposed by Venkatachalam et al [10]. Since experimental evidence [17, 18, 30, 33] indicates the functional importance of intrinsic SOD in determining the renal tissue damage following transient ischemia, we were intrigued by the possibility that the site-selective pattern in the expression of the SOD gene may underlie the distinctive difference between the proximal versus distal tubules in susceptibility to post-ischemic injury. To address this issue, we used a Mn-SOD cDNA probe which was verified previously by Southern blot analysis to be highly specific [34]. Also, Northern blot analyses performed in previous studies [19, 23, 34–36] demonstrated that the probe hybridized all of the five Mn-SOD gene transcripts with sizes ranging from the 1.0 to the 3.8 kb that are expected in rat tissues, thereby verifying its sensitivity. The distinct localization of Mn-SOD mRNA within the

distal tubule observed with this probe in the present study is in concert with the current prevailing notion that, unlike Cu/Zn-SOD, expression of which is largely constitutive, Mn-SOD is inducible and regulated by a number of biologic factors [19–21, 23, 35–37]. In parallel with our present observations at the mRNA level, a previous immunohistochemical study in normal rats [38] documented qualitatively more intense staining of the thick ascending limb with Mn-SOD antibody, when compared to the proximal tubule.

In addition to these baseline patterns of Mn-SOD gene expression, our studies further revealed that an induction of Mn-SOD takes place in a highly cell-specific manner and, again, most prominently in the distal tubule. In this regard, it is often impossible to determine the quantitative importance of the synthesis versus degradation of mRNA for a given alteration in the level of mRNA. Theoretically, the observed widening of the difference between the two segments may reflect an accelerated decay of the mRNA in the proximal tubule secondary to the initial hypoxic insult. A previous *in vivo* study [17], however, indicates otherwise: a progressive increase in renal Mn-SOD activity was observed after ischemia-reperfusion. Thus, the relative predominance of the distal over proximal tubule expression for Mn-SOD mRNA in the present study likely reflects largely enhanced distal tubule expression and not a decrease in the proximal tubules. Further, the enhanced expression of mRNA is followed by an increase in enzyme activity. Our previous observations [17] showed that the time course of the induction of Mn-SOD parallels
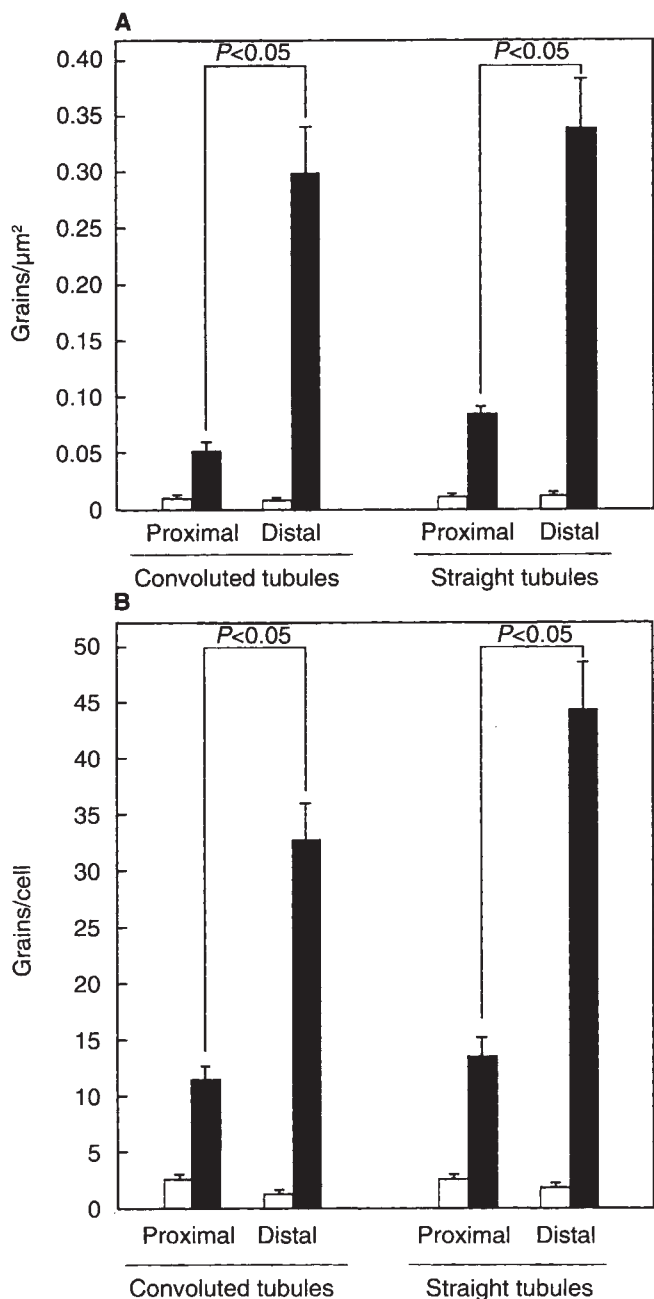
Fig. 8. *Quantitative analysis of Mn-SOD mRNA signals in rat kidneys exposed to a transient ischemia.* Closed bars, density of silver grains in the nephron segments hybridized with antisense cRNA; open bars, those in segments hybridized with sense cRNA. The density of silver grains, expressed as number per area (*upper panel*) and per cell (*lower panel*), was markedly greater in distal than proximal tubules in the superficial cortex (convoluted tubules) and the outer stripe of outer medulla (straight tubules). Difference of the grain densities between the distal and proximal was more remarkable in the kidneys exposed to transient ischemia than in normal undisturbed kidneys (compare to Fig. 6).

development in the kidney of a tolerance to subsequent ischemia-reperfusion injury. Therefore, it is plausible that this further accentuation of the difference in Mn-SOD gene expression after the insult may have played a crucial role in the progressive

structural damage found only in the proximal tubules over time. Results from several recent studies by others are relevant to our findings. Thus, some nephrotoxic agents [39–41], which induce renal tissue injury by increasing reactive oxygen metabolites, were shown to spare distal tubules [42, 43] even when proximal tubules showed extensive necrosis. Andreoli and McAteer [44] recently compared several renal epithelial cell lines for their responsiveness to reactive oxygen metabolite exposure *in vitro*. LLC-PK$_1$, NHK-C and OK cells (derived from the proximal tubule) were found to be clearly more susceptible to oxidant injury than MDCK cells (derived from the distal tubule). These cells were derived from different animal species, however. More convincingly, when isolated perfused rat kidneys were exposed to glucose oxidase, that is, a hydrogen peroxide generating system, more profound and extensive morphologic changes occurred in proximal tubules than distal tubules [45]. These changes were completely prevented by antioxidant treatment. Morphologic [46] and functional [47, 48] damage of mitochondria caused by transient ischemic insult is crucial to the subsequent irreversible cellular injuries. Further, SOD pretreatment of the kidneys exposed to ischemia-reperfusion attenuated the typical histologic tubule injury and prevented lipid peroxidation in cortical mitochondria (but not in crude cortical homoginates) [30]. It, therefore, appears reasonable to speculate that Mn-SOD, a primary mitochondrial antioxidant enzyme, may play a prominent role in the tolerance of renal tubular epithelial cells to ischemia-reperfuion injury.

Despite all this supportive evidence, one may realize that modern technologies still fall short of providing a definitive test for the functional significance of the observed local activation of the Mn-SOD gene *in vivo*. For instance, an assay of enzyme activity in the specific nephron segments studied is not available today. Although our previous renal antioxidant enzyme assays revealed that Mn-SOD, glutathione peroxidase, and catalase activities were all enhanced after ischemia-reperfusion insult [17], the relative functional significance of each of the enzymes is impossible to determine by conventional methodologies. Therefore, the contribution of other intrinsic factors, both antioxidant and non-antioxidant, to the unique tolerance of the distal tubule is still conceivable. In this regard, however, Lash and Tokarz [22] documented in their studies with isolated rat renal tubules that the activities of five other antioxidant enzymes, such as, glutathione disulfide reductase, glutathione peroxidase, glutathione S-transferase, catalase and diaphorase, were, instead, significantly higher in proximal than distal tubule cells. Of note, it was shown that, under anaerobic conditions, distal tubules have a greater glycolytic capacity than proximal tubules [49, 50]. Several key enzymes involved in the glycolytic pathway are present in distal tubules [51, 52]. Nevertheless, studies have shown that anaerobic metabolism is far too insufficient to dampen the decrease in mitochondrial ATP synthesis in anaerobic conditions [53]. Recently, 73-kDa heat-shock protein (HSP) has been shown to distribute predominantly in distal tubules when compared to proximal tubules [54]. Transient ischemia causes accumulation of HSP within the kidney [55]. Moreover, HSP is involved in the process of postischemic cellular recovery [56]. Thus, this protein could be a cooperative factor of Mn-SOD in protecting distal tubules against ischemia-reperfusion injury.

The mechanism for the observed intense localization of Mn-SOD gene expression within the distal tubules is of obvious scientific interest. Since this localization was seen in undisturbed

kidneys, distal tubules appear to be uniquely under constant influence of certain stimulant(s). Given our recent demonstration that the gene of Mn-SOD contains nucleotide sequence(s) responsive to oxidants [19] and the well established notion that oxidants are constant products of the mitochondrial electron transport chain during the production of ATP, the observed high level of Mn-SOD mRNA in the distal tubule may then reflect a high intracellular oxidant level within the distal tubule under normal physiologic conditions. In support of this possibility, higher Na^+-K^+-ATPase activity [11] and mitochondrial density [57] were demonstrated in the distal than in the proximal tubule.

It may be reasonable to conclude that the observed localization and activation of the Mn-SOD gene appear to be strategic by protecting distal tubules from ischemia-reperfusion insult. However, whether this mechanism, indeed, operates *in vivo* and has primary importance for the unique resistance of the distal tubules to several forms of acute injury has not been clarified in the present study. Much technological advancement is required to answer these questions.

Acknowledgments

Reprint requests to Iekuni Ichikawa, M.D., Ph.D., Division of Pediatric Nephrology, Vanderbilt University Medical Center, C-4204 Medical Center North, 21st & Garland Avenue, Nashville, Tennessee 37232-2584, USA.

References

1. GLAUMANN B, GLAUMANN H, BEREZESKY IK, TRUMP BF: Studies on the pathogenesis of ischemic cell injury. II. Morphological changes of the pars convoluta (P1 and P2) of the proximal tubule of the rat kidney made ischemic *in vivo*. *Virchows Arch B Cell Path* 19:281–302, 1975
2. GLAUMANN B, TRUMP BF: Studies on the pathogenesis of ischemic cell injury. III. Morphological changes of the proximal pars recta (P3) of the proximal tubule of the rat kidney made ischemic *in vivo*. *Virchows Arch B Cell Path* 19:303–323, 1975
3. KREISBERG JI, BULGER RE, TRUMP BF, NAGLE RB: Effect of transient hypotension on the structure and function of rat kidney. *Virchows Arch B Cell Path* 22:121–133, 1976
4. DOBYAN DC, NAGLE RB, BULGER RE: Acute tubular necrosis in the rat kidney following sustained hypotension: Physiologic and morphologic observations. *Lab Invest* 37:411–422, 1977
5. ROSEN S, EPSTEIN FH, BREZIS M: Determinants of intrarenal oxygenation: Factors in acute renal failure. *Renal Failure* 14:321–325, 1992
6. SHANLEY PF, ROSEN MD, BREZIS M, SILVA P, EPSTEIN FH, ROSEN S: Topography of focal proximal tubular necrosis after ischemia with reflow in the rat kidney. *Am J Pathol* 122:462–468, 1986
7. BREZIS M, ROSEN S, SILVA P, EPSTEIN FH: Selective vulnerability of the thick ascending limb to anoxia in the isolated perfused rat kidney. *J Clin Invest* 73:182–190, 1984
8. BREZIS M, ROSEN S, SILVA P, EPSTEIN FH: Renal ischemia: A new perspective. *Kidney Int* 26:375–383, 1984
9. SHANLEY PF, BREZIS M, SPOKES K, SILVA P, EPSTEIN FH, ROSEN S: Hypoxic injury in the proximal tubule of isolated perfused rat kidney. *Kidney Int* 29:1021–1032, 1986
10. VENKATACHALAM MA, BERNARD DB, DONOHOE JF, LEVINSKY NG: Ischemic damage and repair in the rat proximal tubule: differences among the S1, S2, and S3 segments. *Kidney Int* 14:31–49, 1978
11. KATZ AI, DOUCET A, MOREL F: Na^+-K^+-ATPase activity along the rabbit, rat, and mouse nephron. *Am J Physiol* 237:F114–F120, 1979
12. BRAAM B, MITCHELL KD, KOOMANS HA, NAVAR LG: Relevance of the tubuloglomerular feedback mechanism in pathophysiology. *J Am Soc Nephrol* 4:1257–1274, 1993
13. THURAU K, BOYLAN JW: Acute renal success: The unexpected logic of oliguria in acute renal failure. *Am J Med* 61:308–315, 1976
14. KRIZ W, KAISSLING B: Structural organization of the mammalian kidney, in The Kidney: *Physiology and Pathophysiology*, edited by SELDIN DW, GIEBISCH G, New York, Raven Press, 1992, pp 707–767
15. VENKATACHALAM MA, KRIZ W: Anatomy, in *Pathology of the Kidney*, edited by HEPTINSTALL RH, Boston, Little, Brown & Co., 1992, pp 1–92
16. KAWAMURA T, YOSHIOKA T, BILLS T, FOGO A, ICHIKAWA I: Glucocorticoid activates glomerular antioxidant enzymes and protects glomeruli from oxidant injuries. *Kidney Int* 40:291–301, 1991
17. YOSHIOKA T, BILLS T, MOORE-JARRETT T, GREENE HL, BURR IM, ICHIKAWA I: Role of intrinsic antioxidant enzymes in renal oxidant injury. *Kidney Int* 38:282–288, 1990
18. SHANLEY P, WHITE CW, AVRAHAM K, GRONER Y, BURKE TJ: Renal ischemia-reperfusion in transgenic mice with endogenous high levels of superoxide dismutase (SOD). (abstract) *J Am Soc Nephrol* 1:604, 1990
19. YOSHIOKA T, HOMMA T, MEYRICK B, TAKEDA M, VAN DER MEER R, MOORE-JARRETT T, ICHIKAWA I: Oxidants induce transcriptional activation of manganese superoxide dismutase in glomerular cells. *Kidney Int* 46:405–413, 1994
20. HO YS, HOWARD AJ, CRAPO JD: Molecular structure of a functional rat gene for manganese-containing superoxide dismutase. *Am J Respir Cell Mol Biol* 4:278–286, 1991
21. KRALL J, BAGLEY AC, MULLENBACH GT, HALLEWELL RA, LYNCH RE: Superoxide mediates the toxicity of paraquat for cultured mammalian cells. *J Biol Chem* 263:1910–1914, 1988
22. LASH LH, TOKARZ JJ: Oxidative stress in isolated rat renal proximal and distal tubular cells. *Am J Physiol* 259:F338–F347, 1990
23. DOUGALL WC, NICK HS: Manganese superoxide dismutase: A hepatic acute phase protein regulated by interleukin-6 and glucocorticoids. *J Endocrinol* 129:2376–2384, 1991
24. COX KH, DELEON DV, ANGERER LM, ANGERER RC: Detection of mRNAs in sea urchin embryos by *in situ* hybridization using asymmetric RNA probes. *Dev Biol* 101:485–502, 1984
25. KAKINUMA Y, FOGO A, INAGAMI T, ICHIKAWA I: Intrarenal localization of angiotensin II type 1 receptor mRNA in the rat. *Kidney Int* 43:1229–1235, 1993
26. LIU L, DUNN T, CHRISTAKOS S, PAINTON OH, BOURDEAU JE: Calbindin-D_{28k} gene expression in the developing mouse kidney. *Kidney Int* 44:322–330, 1993
27. BIRD JE, MIHOAN K, WILSON CB, YOUNG SG, MUNDY CA, PARTHASARATHY S, BLANTZ RC: Ischemic acute renal failure and antioxidant therapy in the rat. *J Clin Invest* 81:1630–1638, 1988
28. BREYER MD, JACOBSON HR, DAVIS LS, BREYER RM: *In situ* hybridization and localization of mRNA for the rabbit prostaglandin EP_3 receptor. *Kidney Int* 43:1372–1378, 1993
29. NOLAND TD, CARTER CE, JACOBSON HR, BREYER MD: PGE_2 regulates cAMP production in cultured rabbit CCD cells: Evidence for dual inhibitory mechanisms. *Am J Physiol* 263:C1208–C1215, 1992
30. PALLER MS, HOIDAL JR, FERRIS TF: Oxygen free radicals in ischemic acute renal failure in the rat. *J Clin Invest* 74:1156–1164, 1984
31. BECKMAN JK, YOSHIOKA T, KNOBEL SM, GREENE HL: Biphasic changes in phospholipid hydroperoxide levels during renal ischemia/reperfusion. *Free Rad Biol Med* 11:335–340, 1991
32. HEYMAN SN, BREZIS M, EPSTEIN FH, SPOKES K, ROSEN S: Effect of glycine and hypertrophy on renal outer medullary hypoxic injury in ischemia reflow and contrast nephropathy. *Am J Kidney Dis* 19:578–586, 1992
33. BAKER GL, CORRY RJ, AUTOR AP: Oxygen free radical induced damage in kidneys subjected to warm ischemia and reperfusion. Protective effect of superoxide dismutase. *Ann Surg* 202:628–641, 1985
34. HURT J, HSU JL, DOUGALL WC, VISNER GA, BURR IM, NICK HS: Multiple mRNA species generated by alternate polyadenylation from the rat manganese superoxide dismutase gene. *Nucl Acid Res* 20:2985–2990, 1992
35. VISNER GA, DOUGALL WC, WILSON JM, BURR IM, NICK HS:

Regulation of manganese superoxide dismutase by lipopolysaccharide, interleukin-1, and tumor necrosis factor: Role in the acute inflammatory response. *J Biol Chem* 265:2856–2864, 1990

36. YOSHIOKA T, KAWAMURA T, MEYRICK BO, BECKMAN JK, HOOVER RL, YOSHIDA H, ICHIKAWA I: Induction of manganese superoxide dismutase by glucocorticoids in glomerular cells. *Kidney Int* 45:211–219, 1994

37. WONG GHW, GOEDDEL DV: Induction of manganese superoxide dismutase by tumor necrosis factor: Possible protective mechanism. *Science* 242:941–944, 1988

38. DOBASHI K, ASAYAMA K, HAYASHIBE H, UCHIDA N, KOBAYASHI M, KAWAOI A, KATO K: Effect of diabetes mellitus induced by streptozotocin on renal superoxide dismutases in the rat. *Virchows Archiv B Cell Pathol* 60:67–72, 1991

39. WALKER PD, SHAH SV: Evidence suggesting a role for hydroxl radical in gentamycin-induced acute renal failure in rats. *J Clin Invest* 81:334–341, 1988

40. SUGIYAMA S, HAYAKAWA M, KATO T, HANAKI Y, SHIMIZU K, OZAWA T: Adverse effects of anti-tumor drug, cisplatin, on rat kidney mitochondria: disturbances in glutathione peroxidase activity. *Biochem Biophys Res Comm* 159:1121–1127, 1989

41. BAUD L, ARDAILLOU R: Reactive oxygen species: Production and role in the kidney. *Am J Physiol* 251:F765–F776, 1986

42. HOUGHTON DC, HARTNETT M, CAMPBELL-BOSWELL M, PORTER G, BENNETT W: A light and electron microscopic analysis of gentamycin nephrotoxicity in rats. *Am J Pathol* 82:589–612, 1976

43. DOBYAN DC, JOSEPH L, JACOBS C, KOSEK J, WEINER MW: Mechanism of cis-platinum nephrotoxicity: II. Morphologic observations. *J Pharmacol Exp Ther* 213:551–556, 1980

44. ANDREOLI SP, MCATEER JA: Reactive oxygen molecule-mediated injury in endothelial and renal tubular epithelial cells *in vitro*. *Kidney Int* 38:785–794, 1990

45. LINAS SL, SHANLEY PF, WHITE CW, PARKER NP, REPINE JE: O_2 metabolite-mediated injury in perfused kidneys is reflected by consumption of DMTU and glutathione. *Am J Physiol* 253:F692–F701, 1987

46. GLAUMANN B, GLAUMANN H, TRUMP BF: Studies of cellular recovery from injury. III. Ultrastructual studies on the recovery of the pars recta of the proximal tubule (P_3 segment) of the rat kidney from temporary ischemia. *Virchows Arch B Cell Path* 25:281–308, 1977

47. MERGNER WJ, SMITH MW, TRUMP BF: Studies on the pathogenesis of ischemic cell injury. *Virchows Archiv B Cell Pathol* 26:17–26, 1977

48. WILSON DR, ARNOLD PE, BURKE TJ, SCHRIER RW: Mitochondrial calcium accumulation and respiration in ischemic acute renal failure in the rat. *Kidney Int* 25:519–526, 1984

49. ENDOU H, JUNG KY: Heterogeneity of nephron energy metabolism: Implications for response to hypoxic insult, in *Nephrology*, edited by HATANO M, Tokyo, Springer-Verlag, 1991, pp 665–672

50. BASTIN J, CABON N, THOMPSON M, LOWRY OH: Change in energy reserves in different segments of the nephron during brief ischemia. *Kidney Int* 31:1239–1247, 1987

51. SCHMIDT U, MAROSVARI J, DUBACH UC: Renal metabolism of glucose: Anatomical site of hexokinase activity in the rat nephron. *FEBS Lett* 53:26–28, 1975

52. SCHMID H, MALL A, SCHOLZ M, SCHMIDT U: Unchanged glycolytic capacity in rat kidney under conditions of stimulated gluconeogenesis. Determination of phosphofructokinase and pyruvate kinase in micro-dissected nephron segments of fasted and acidotic rats. *J Physiol Chem* 361:819–827, 1980

53. UCHIDA S, ENDOU H: Substrate specificity to maintain cellular ATP along the mouse nephron. *Am J Physiol* 255:F977–F983, 1988

54. KOMATSUDA A, WAKUI H, IMAI H, NAKAMOTO Y, MIURA AB, ITOH H, TASHIMA Y: Renal localization of the constitutive 73-kDa heat-shock protein in normal and PAN rats. *Kidney Int* 41:1204–1212, 1992

55. EMAMI A, SCHWARTZ JH, BORKAN SC: Transient ischemia or heat stress induces a cytoprotectant protein in rat kidney. *Am J Physiol* 260:F479–F485, 1991

56. CURRIE RW, KARMAZYN M, KLOC M, MAILER K: Heat-shock response is associated with enhanced postischemic ventricular recovery. *Circ Res* 63:543–549, 1988

57. PFALLER W, RITTINGER M: Quantitative morphology of the rat kidney. *Int J Biochem* 12:17–22, 1980